Resonant Tunnelling Diode Terahertz Sources for Broadband Wireless Communications

Edward Wasige and Jue Wang

School of Engineering, University of Glasgow, Rankine Bldg, Oakfield Avenue, Glasgow G12 8LT

This paper presents monolithic microwave/millimeter-wave integrated circuit (MMIC) resonant tunneling diode (RTD) oscillators with high performance: high power at high (terahertz) frequencies. The circuit topology employs two $In_{0.53}Ga_{0.47}As/AlAs$ RTDs in parallel and each device is biased individually. These oscillators operate at 125GHz, 156GHz and 166 GHz with output power 0.34 mW, 0.24 mW and 0.17 mW respectively. These are highest power reported for RTD oscillator in D-band (110 GHz-170 GHz) frequency range. The phase noise of the RTD oscillators was characterized and is reported. This work demonstrates the circuit-based RTD oscillator design approach to increase the output power of RTD oscillators at millimeter-waves. The designs are being revised for higher output powers and now also being scaled into the terahertz frequency range proper.

INTRODUCTION

Terahertz (THz) technology has attracted arising interest because of the enormous emerging applications in such as security imaging systems, ultrafast wireless communication systems, bio/molecular spectroscopy research and high resolution radar, etc. [1]. Because of the lack of coherent THz sources, particularly with high output power level, compact size, room-temperature operation, there is a THz gap covering the transition frequency band from traditional electronics to photonics. Traditional electronic devices like CMOS, heterojuction bipolar transistors (HBTs) and high electron mobility transistors (HEMTs) are limited by the cut-off frequency. Two terminal electronic devices such as impact ionization transit-time (IMPATT) diodes [2], tunnel-injection transit-time (TUNNETT) diodes [3], and transferred-electrons (Gunn) diodes [4] are therefore being developed to bridge the gap. Among these solid state devices, RTDs exhibit the highest oscillation frequency. The published highest frequency of single device RTD oscillator is 1.55 THz with 0.4 μW output power [5]. Optical devices like far-infrared (FIR) gas laser and quantum cascade lasers (QCLs) are also being developed to cover the frequencies over 1 THz. For gas lasers, the bulky system often requires cryogenic cooling which also increase the cost. For QCL, to realize long wavelength (below 1 THz) becomes challenging because of the extremely small intersubband energy separation [6]. RTDs are one of the most promising solid-state terahertz (THz) sources operating at room temperature, even though their output power remains low, in the tens of micro-Watts range or less.

In this paper, integrated circuit RTD oscillators in the D-band with record high power are reported. The circuit-based RTD oscillator design approach was first demonstrated in a hybrid microstrip circuit at low microwave frequencies [7]. Later, 28 GHz and 76 GHz RTD oscillators with around 1 mW were first realized by the authors [8][9]. By improving the circuit design,

three different RTD oscillators which work in D-band frequencies 125GHz, 156GHz and 166 GHz, with output power of 0.34 mW, 0.24 mW, 0.17 mW, respectively, were fabricated and characterized [10]. This and on-going related work is expected to lead to high power RTD oscillators operating in the 100 GHz – 1 THz range with output power of at least 1 mW.

DEVICE STRUCTURE & FABRICATION

An RTD device consists of a narrow band gap semiconductor material sandwiched between two thin wide band gap materials as illustrated in Fig 1(a) for InP-based RTDs. In the work reported here, a 4.5 nm $In_{0.53}Ga_{0.47}As$ quantum well is sandwiched between two 1.4 nm thick AlAs barriers. The InGaAs/AlAs heterostructure was grown by molecular beam epitaxy (MBE) on a semi-insulating InP substrate. The collector layer and emitter layers are each 80nm thick of $In_{0.53}Ga_{0.47}As$ which are doped ($2\times10^{18}cm^{-3}$) with silicon. The structure is completed with highly doped ($3\times10^{19}cm^{-3}$: Si) contact layers on either side.

The devices were fabricated using optical lithography to define the required patterns. There are two different mesa sizes 3×5 μm^2 and 5×5 μm^2 which were defined by H_3PO_4: H_2O_2:H_2O wet etching. The mesas were passivated by polyimide PI-2545. A micrograph picture of the completed RTD device is shown in Fig. 1 (b). The measured IV characteristic of the 3×5 μm^2 and 5×5 μm^2 sized RTD single device is shown in Fig. 2. It is noted that for these devices the peak current density was around 73 kA/cm^2 and the peak to valley current ratio (PVCR) was about 1.8. The peak to valley current (ΔI) and voltage (ΔV) differences determine the maximum RF power that could be delivered by a device when employed in an oscillator circuit which is given by $3\Delta I \Delta V/16$ [11].

For a given material structure, the peak-to-valley voltage difference ΔV and the peak-to-valley current density ΔJ are fixed, and so for a chosen value of the stabilising resistance, R_e, the maximum RTD device size, A_{max}, can be calculated using [11]:

$$A_{max}R_e = \frac{2\Delta V}{3\Delta J}$$

The use of the largest permissible device sizes, i.e. devices which can be stabilised at DC or low frequencies, enables the realisation of RTD oscillators delivering the highest possible RF powers [11].
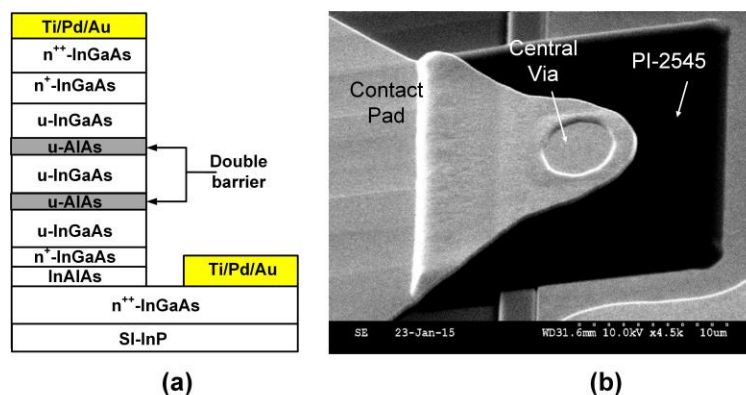
Fig 1. (a) Schematic layer structure of an RTD device. (b) Micrograph of the fabricated 5×5 μm^2 RTD device.
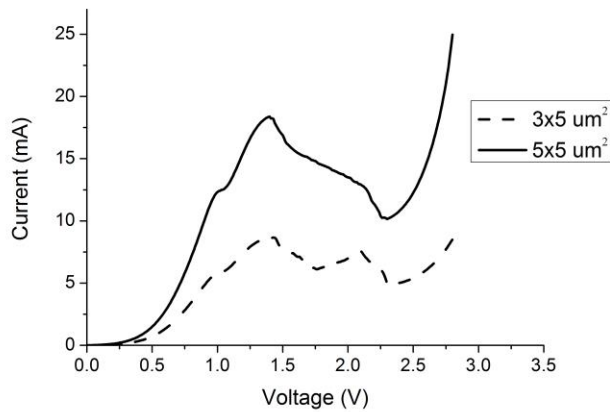
Fig 2. Measured I-V characteristic of the fabricated 3×5 μm^2 (dash line) and 5×5 μm^2 (solid line) RTD.

2-RTD OSCILLATOR TOPOLOGY & DESIGN

The RTD oscillator design approach presented here employs two RTDs in parallel as shown in Fig. 3 (a). With this topology, twice the RF output power of a single device RTD oscillator can be obtained. Each of the RTDs is biased individually with its own shunt resistor R_e to suppress the low frequency bias oscillations and a bypass capacitor C_e to short-circuit the RF signal to ground avoiding RF power dissipating over R_e [7].Inductor L is designed to resonate with RTD self-capacitances to obtain the desired frequency. R_L is the load resistance. The small signal equivalent circuit of the circuit of Fig. 3 (a) is shown in Fig. 3 (b). Each RTD is modelled by its lumped equivalent circuit model which is the negative differential conductance - G_{1n}/- G_{2n} in parallel with the self-capacitance C_{1n}/C_{2n}. For the used layer structure, the nominal device geometrical self-capacitance is 2.1 fF/μm^2.

The circuit was realised in integrated form. Thin film NiCr resistors were used to realise the stabilising resistors R_e., while the bypass capacitors C_e were realized as metal-insulator-metal (MIM) capacitors. For the MIMs, a thin dielectric layer Si_3N_4 (75 nm) was deposited by inductively coupled plasma (ICP) chemical vapor deposition (CVD). The inductor L is realised by a short-circuited coplanar waveguide (CPW) stub, the short-circuit being though the bypass capacitor C_e in this case. R_L was introduced by the impedance of spectrum analyzer which is usually 50Ω. A photograph of the fabricated oscillator is shown in Fig. 4
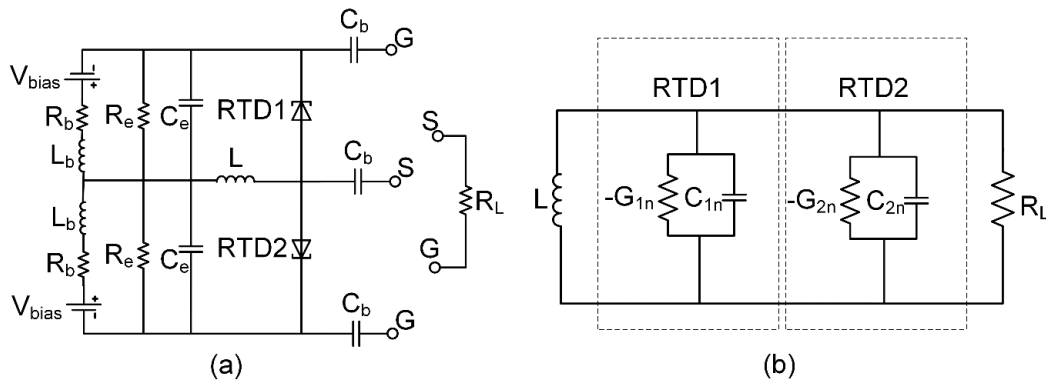
Fig 3. (a) Two RTD oscillator schematic circuit. Each RTD is biased individually with its own DC stabilization circuit R_e and C_e. (b) Oscillator RF equivalent circuit excluding the device parasitic elements.
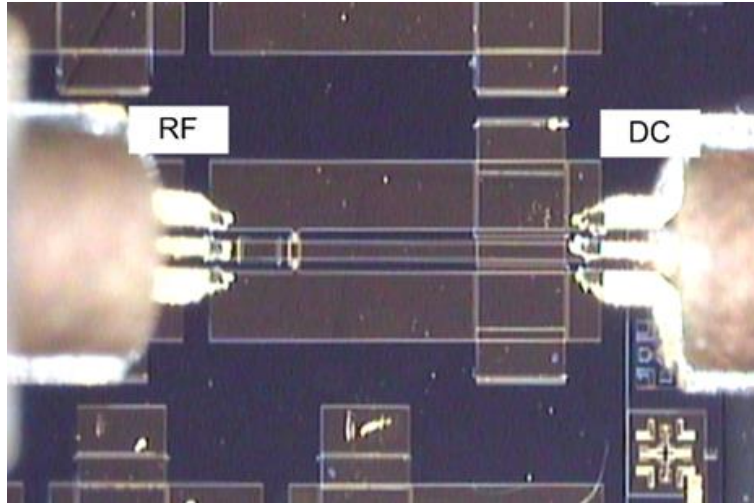
Fig 4. Photograph of the fabricated oscillator that employs 2 RTD devices during characterisation with measurement probes landed on the chip.

MEASUREMENT RESULTS

The oscillators were characterized on-wafer by using Agilent E4448A spectrum analyzer. The schematic diagram of the measurement setup is shown in Fig 5(a). The oscillators were biased through GSG Cascade probe, while a WR-06 GSG Picoprobe was used to probe their outputs. The measured signal was mixed down by using D-band harmonic mixer from Farran Technology. A 2.5 mm coax cable was used to connect the mixer and diplexer. The diplexer is used to separate the local oscillator (LO) and intermediate frequencies (IF). With the build in signal identification function of the spectrum analyzer, the oscillation frequency can be accurately identified. The output power was first noted from the spectrum analyser by considering the typical conversion loss of the mixer, ~55 dB. The oscillator output was then measured directly using a power meter, the Erikson PM4. Since the input of power sensor head is WR-10 (W-band) waveguide, a WR-6 to WR-10 tapered waveguide was used as shown in Fig. 5(b). The reported output powers were corrected for the 3 dB insertion loss that is specified by the manufacturer for this setup.

Measurement results from two different device sizes, 3×5 µm^2 and 5×5 µm^2, with two different CPW lengths, 20 µm and 30 µm, aiming at different frequencies are reported here. The 125 GHz oscillator had a 5×5 µm^2 device and 30 µm long line, and provided 0.68 mW (-1.7 dBm) output power after compensating for the insertion loss. The 156 GHz oscillator had a smaller 3×5 µm^2 device but also a 30 µm long CPW line, and provided 0.47 mW (-3.3 dBm) output power, while the 166 GHz oscillator had also a 3×5 µm^2 device but a shorter 20 µm long CPW line, and provided 0.34 mW (-4.7 dBm) output power. The measured spectra and frequency with bias for the 166 GHz oscillator is shown in Figures 6 and 7, respectively. The oscillation frequency reduces wih bias even though the range is very limited (Fig. 6).

The phase noise of 125 GHz and 156 GHz RTD oscillators was measured directly by build-in phase noise function of Agilent spectrum analyser E4448A. For the 125 GHz signal the phase noise was -79 dBc/Hz @ 1 MHz and -92 dBc/Hz @10 MHz offset (plot not shown), while for the 156 GHz signal it was -63 dBc/Hz @ 1 MHz and -83 dBc/Hz @10 MHz offset as shown in Fig. 8, respectively. Due to the high conversion loss of the harmonic mixer, the detected output power at 166 GHz was low, and it was difficult to measure the phase noise.

The results are summarized in Table 1, which also includes comparable oscillator results of Si-based technologies [12-13]. It is clear that Si technologies for these require very fine sub-micron or even sub-100nm features for these kind of oscillators. However, the present RTD oscillators dissipate larger DC powers due to the shunt resistor required for bias stabilisation, and so this is an area that requires new innovation in terms of RTD device and circuit design.

RTD TERAHERTZ SOURCES

Fig. 10 shows a comparison of the output power versus frequency of recently published RTD sources [14]. The frequency coverage beyond 1 THz is clear to see but also the low output power is apparent. The major challenge for the RTD technology in becoming a THz electronics platform therefore lies in increasing the output power to over 1 mW across the 0.1-1 THz range. Fig. 10 also shows the simulated output power of an optimal/idealised single RTD oscillator using the device data from Ref. [15] and using the RTD output power analysis described in Ref. [11]. The simulated results indicate the potential of RTDs to meet the output power challenge, but further research in improved device/circuit design is necessary.

RTD OPTOELECTRONICS

Resonant tunnelling diodes (THz sources) can be designed as photo-diodes and can be integrated with laser diodes to pursue the development of a unified technology that can be integrated into both ends of the optical and wireless links [16-17]. The target application area is consumer portable devices and fibre-optic supported base-stations to enable the deployment of 10 Gbps short-range wireless communication devices in the short term and paving the way for 100 Gbps in the long term, seamlessly integrated with optical fibre networks [18].

CONCLUSION

Relatively high power and low phase noise resonant tunneling diode D-band free-running oscillators with simple fabrication requirements have been described. The negative differential resistance (NDR) region for the devices lies in the 1.4 V (peak voltage) to 2.3 V (valley voltage) range and so high bias voltages are required. 50-Ω Oscillator loads rather than optimal loads were used in the designs, and the (significant) mismatch reduced the output power levels. Future work will aim for improved circuit design, i.e. realise optimally loaded oscillators. Also, research into new power combining topologies, e.g. based on synchronisation, promises higher output oscillator powers. Modulation bandwidths of RTD oscillators of up to 30 GHz have been recently demonstrated by Japanese researchers, demonstrating the potential of this technology for broadband wireless communications [19].
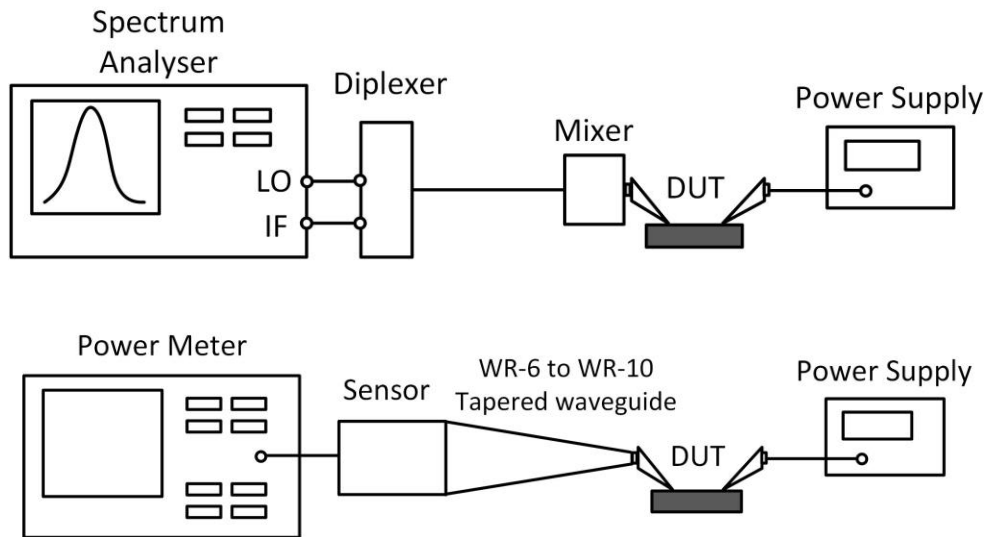
Fig 5. Schematic diagram (a) on-wafer spectrum measurement - top. (b) Power measurement setup for D-band frequencies – bottom.
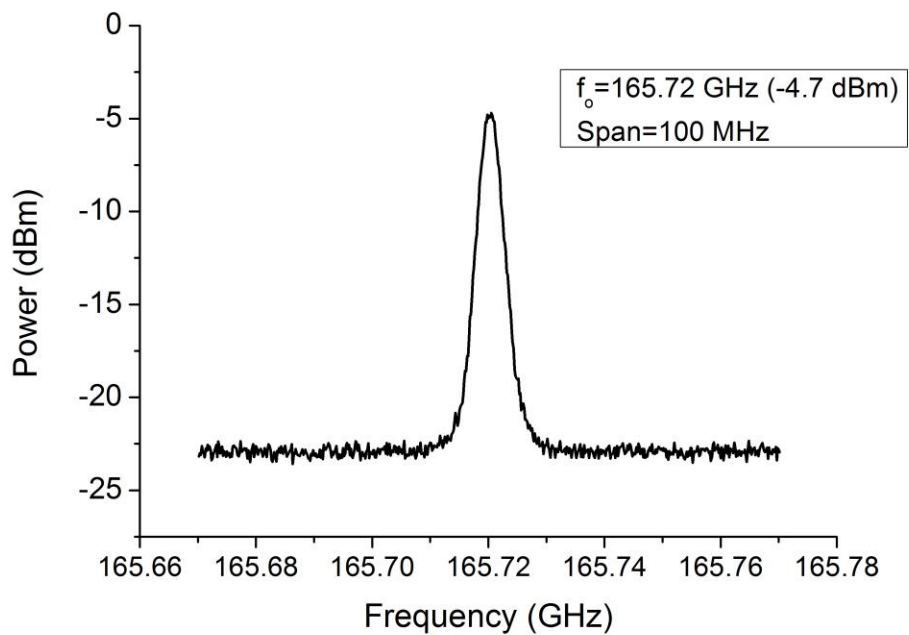
Fig 6. Measured spectrum of the 166 GHz oscillator when V_{bias} = 1.70V, I_{bias} = 112.8 mA
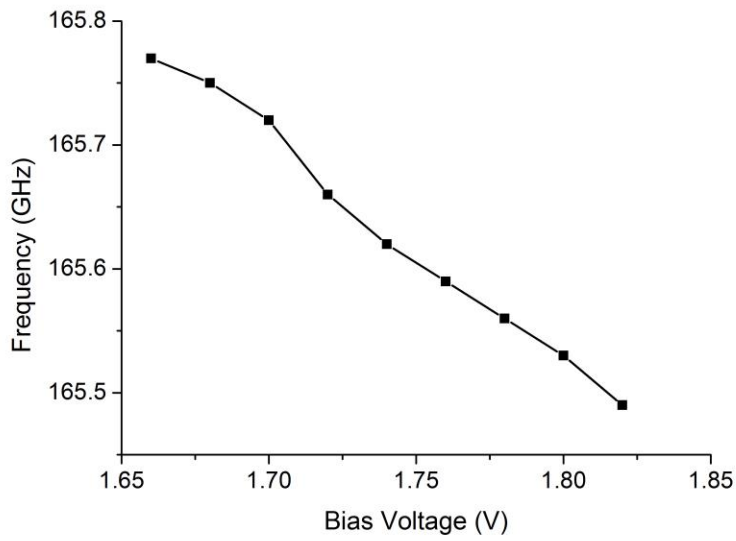
Fig 7. Measured frequency versus bias voltage for the 166 GHz oscillator
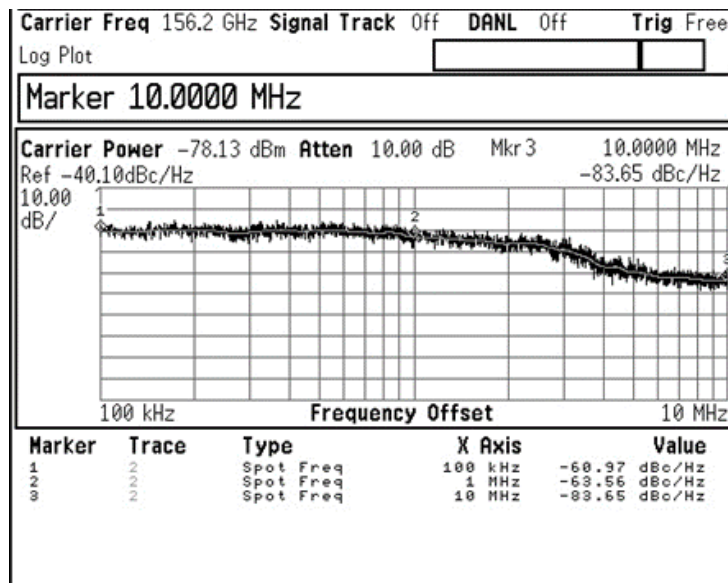
Fig 8. Measured phase noise of the 156 GHz oscillator RTD oscillator
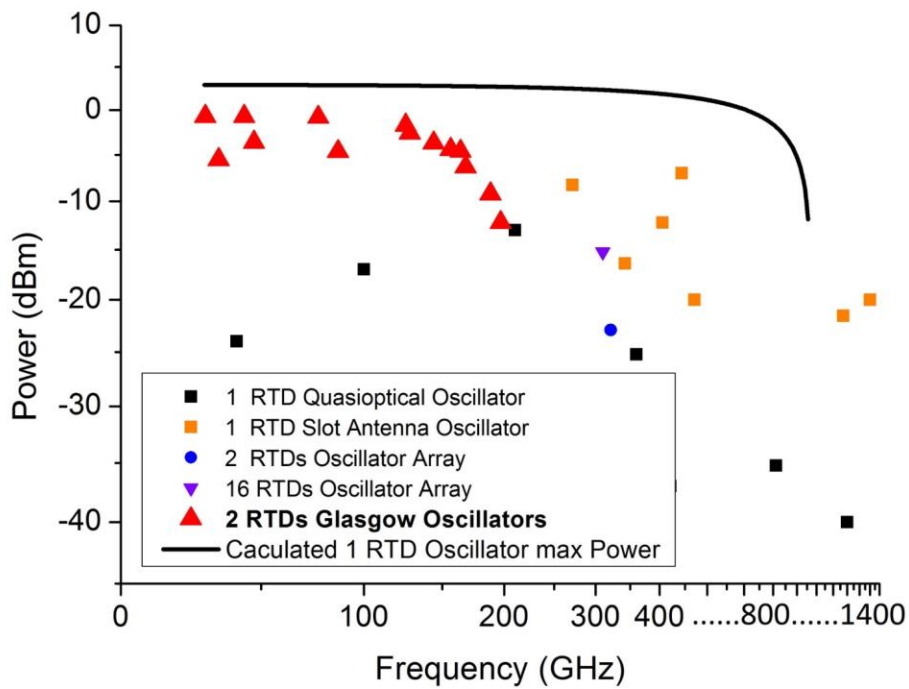
Fig 9. (a) Two RTD oscillator schematic circuit. Each RTD is biased individually with its own DC stabilization circuit R_e and C_e. (b) Oscillator RF equivalent circuit excluding the device parasitic elements.

Table 1: Summary of perfomance of D-band RTD oscillators.

Device size (μm²) or technology node (nm)	CPW length (μm)	Freq. (GHz)	Power (dBm/mW)	Phase noise (dBc/Hz)	DC Power (mW)	Reference
5×5 μm²	30	125	-1.7/0.68	-79@1MHz -92@10 MHz	415	This work
3×5 μm²	30	156	-3.3/0.47	-63@1MHz -83@10 MHz	374	This work
3×5 μm²	20	166	-4.7/0.34	n/a	191	This work
130 nm	n/a	154	7/	-87@1MHz	68	[11]
90 nm	n/a	140	-19/	-85@2MHz	96	[12]

REFERENCES

1. P.H. Siegel, "Terahertz technology," IEEE Transactions on Microwave Theory and Techniques, vol.50, no.3, pp.910-928, Mar 2002.

2. K. Chang, W.F. Thrower, and G.M. Hayashibara, "Millimeter-Wave Silicon IMPATT Sources and Combiners for the 110-260 GHz Range," IEEE Transactions on Microwave Theory and Techniques, vol.29, no.12, pp.1278-1284, Dec 1981.

3. J. Nishizawa, P. Plotka, T. Kurabayashi, and H. Makabe, "706 GHz GaAs CW fundamental-mode TUNNETT diodes fabricated with molecular layer epitaxy," Physca Status Solidi, vol 5, pp 2802–2804, 2008.

4. A. Khalid, C. Li, V. Papageogiou, G.M. Dunn, M.J. Steer, I.G. Thayne, M. Kuball, C.H. Oxley, M. Montes Bajo, A. Stephen, J. Glover, and D.R.S. Cumming, "In0.53Ga0.47As Planar Gunn Diodes Operating at a Fundamental Frequency of 164 GHz," IEEE Electron Device Letters, vol.34, no.1, pp. 39-41, Jan. 2013.

5. T. Maekawa, H. Kanaya, S.Suzuki, M. Asada, " Frequency increase in terahertz oscillation of resonant tunnelling diode up to 1.55 THz by reduced slot-antenna length," Electronics Letters , vol.50, no.17, pp.1214-1216, 2014.

6. B.S. Williams, S. Kumar, Q. Hu, J.L. Reno, "Resonant-phonon terahertz quantum-cascade laser operating at 2.1 THz (λ≃141 μm)," Electronics Letters, vol.40, no.7, pp.431-433, 2004.

7. L. Wang and E. Wasige, "Tunnel diode microwave oscillators employing a novel power combining circuit topology," European Microwave Conference (EuMC), pp. 1154-1157, Sept. 2010.

8. J. Wang, L. Wang, C. Li, B. Romeira, and E. Wasige, "28 GHz MMIC Resonant Tunneling Diode Oscillator of around 1mW Output Power," Electronics letters, vol. 49, No.13, , pp. 816-818. 2013

9. J. Wang, L. Wang, C. Li, K. Alharbi, A. Khalid and E. Wasige, "W-band InP-based Resonant Tunnelling Diode Oscillator with Milliwatt Output Power," The 26th International Conference on Indium Phosphide and Related Materials, Montpellier, France, May, 2014.

10. J. Wang, A. Alharbi, A. Ofiare, H. Zhou, Ata Khalid, D. Cumming and E. Wasige, "High performance resonant tunnelling diode oscillators for THz applications," Compound Semiconductor IC Symposium, 11-14 October 2015, New Orleans, USA.

11. L. Wang, "Reliable design of tunnel diode and resonant tunnelling diode based microwave and millimeterwave sources," PhD Thesis, University of Glasgow, 2010.

12. S. Zeinolabedinzadeh, P. Song, M. Kaynak, M. Kamarei, B. Tillack, J. D. Cressler, "Low phase noise and high output power 367 GHz and 154 GHz signal sources in 130 nm SiGe HBT technology," IEEE MTT-S International Microwave Symposium, pp.1-4, 2014.

13. C. Changhua, K.K.O,"A 140-GHz fundamental mode voltage-controlled oscillator in 90-nm CMOS technology," Microwave and Wireless Components Letters, vol.16, no.10, pp.555-557, 2006

14. J. Wang, "Monolithic microwave/millimetrewave integrated circuit resonant tunnelling diode sources with around a milliwatt output power," PhD Thesis, University of Glasgow, 2014.

15. M. Asada, S. Suzuki and N. Kishimoto, "Resonant tunnelling diodes for subterahertz and terahertz oscillators," Japanese Journal of Applied Physics, vol. 47, no. 6, pp. 4375-4384, 2008.

16. T.J. Slight, B. Romeira, L. Wang, J.M.L. Figueiredo, E. Wasige, and C.N. Ironside, "A liénard oscillator resonant tunnelling diode-laser diode hybrid integrated circuit: model and experiment," IEEE Journal of Quantum Electronics, 44 (12), 2008. pp. 1158-1163.

17. B. Romeira, J. M. L. Figueiredo, T. J. Slight, L.Wang, E. Wasige, C. N. Ironside, "Nonlinear Dynamics of Resonant Tunneling Optoelectronic Circuits for Wireless/Optical Interfaces," IEEE Journal of Quantum Electronics, Vol.45, 11, 2009, pp.1436-1445.

18. http://ibrow-project.eu/

19. Y. Ikeda, S. Kitagawa, K. Okada, S. Suzuki, M. Asada, "Direct intensity modulation of resonant-tunneling-diode terahertz oscillator up to ~30GHz," IEICE Electronics Express 12, January 2015, p. 20141161.